Mu-Analysis Based Controller Architecture Evaluation for the Fuel Processor in a Fuel Cell Powerplant

Subbarao Varigonda, Mihai Huzmezan, Jonas Eborn, Scott A. Bortoff
United Technologies Research Center, East Hartford, CT 06108, USA.

***Abstract*— Fuel cell power plants with an integrated fuel processing system for hydrogen generation are an attractive option for stationary, distributed power generation. We consider a PEM fuel cell power plant with CPO based fuel processor for generating hydrogen from natural gas. During load transients, the temperatures at various points of the fuel processor need to controlled tightly so that the catalytic reactors function properly. The control of the CPO reactor temperature is particularly challenging due to the highly exothermic oxidation reactions, short residence time and the sensitivity to stoichiometry. We consider two architectures for the CPO exit gas temperature control: the first is a baseline controller designed using a decentralized approach and the second is an advanced controller, designed using multivariable control approach. The advanced controller gives better decoupling and disturbance rejection performance. We employ μ analysis to study the robust stability and robust performance of the two controllers. This analysis shows that the advanced controller is superior. Using the notion of skewed-μ, we establish that, for a prescribed level of performance degradation, the worst-case uncertainty that can be tolerated by the advanced controller is higher than the baseline controller.**

I. Introduction

The fuel processing system (FPS) is an integral part of a fuel cell power plant in applications where hydrogen storage is not a viable option. The FPS reforms a hydrocarbon fuel such as natural gas into a hydrogen rich gas. The reforming is performed using one of the three pathways: catalytic partial oxidation (CPO), catalytic steam reforming (CSR) or autothermal reforming (ATR). A water-gas shift (WGS) reactor is also employed to convert CO to H_2 by reacting with H_2O. In PEM (polymer electrolyte membrane) fuel cell power plants, the FPS includes further reaction stages to bring down the CO content to less than 20 ppm since CO is a poison to the electrode catalyst of the fuel cell. An overview of fuel cell technology and further details on fuel processing can be found in [1]–[4].

A schematic of the FPS using catalytic partial oxidation (CPO or CPOX) reactor is shown in Figure 1. Natural gas fuel is mixed with air and passed to the CPOX reactor. The reformate stream from CPOX containing predominantly H_2, CO, CO_2, H_2O and N_2 is cooled by injecting water and sent to the WGS reactors to remove the bulk of CO and to supplement H_2 production. The reformate from WGS reactors is cooled and mixed with air for further CO clean up in the preferential oxidation (PROX) reactors before being fed to the PEM fuel cell.

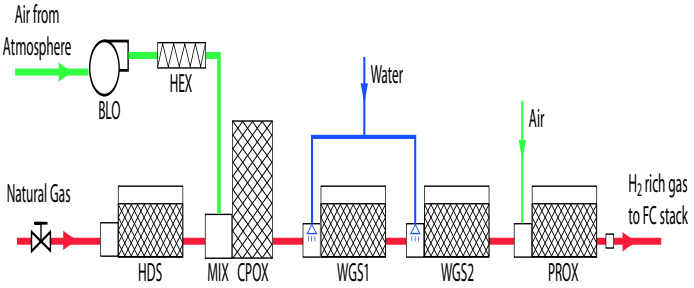

Fig. 1. Schematic of a CPO based fuel processing system in a fuel cell power plant

Fuel cell power plants used in transportation applications and in grid-independent stationary applications are required to follow varying electrical loads. During transients, reactant delivery to the fuel cell stack needs to be properly controlled to prevent starvation and subsequent damage to the stack. The air delivery system on the cathode side is relatively simpler and the hydrogen delivery from the FPS to the anode is typically the key factor limiting the transient capability of the power plant. The control of the FPS during transients involves maintaining proper stoichiometry and operating temperatures for all the reactors. Although CPO based FPS is considered simpler due to higher efficiency and simpler overall system design (*e.g.*, no steam generation required for CPO), the temperature regulation of the CPO reactor during transients presents a significant challenge due to the short residence time, highly exothermic side reaction and the difficulty in measuring the reactor bed temperature.

The control of fuel and air flows into the FPS to regulate the CPO reactor temperature and H_2 delivery to the fuel cell stack has been studied using coarse, system level dynamic models in [5], [6]. In this paper, we describe the application of robust control techniques, in particular, the μ-analysis to study the robustness of different fuel and air control architectures for CPO temperature regulation. We first present an overview of the μ analysis and synthesis framework in Section II and then discuss the application to CPO reactor temperature control in Section III. The conclusions are offered in Section IV.

II. μ Analysis and Synthesis

We now present a brief overview of key concepts from modern robust control theory, including the μ analysis and

synthesis framework for robustness analysis and robust controller design. A detailed exposition of multivariable robust control theory can be found in standard text books such as [7], [8].

A. Model uncertainty and the structured singular value (μ)

Robust control theory offers a framework to systematically account for model uncertainty in the control design process. In the case of a dynamic plant model, uncertainty takes different forms. Determining the plant uncertainty set is equivalent to a quantification of what we know about what we do not know. If this quantification takes a mathematical form then it can be further exploited in analysis and design procedures such as the μ analysis and synthesis. Typical sources of uncertainty are: i) model parameters known approximately or even with errors, ii) plant nonlinearity associated with varying model parameters, iii) imperfect sensors and actuators, and iv) lack of model knowledge in the high frequency range.

Structured uncertainty is parametric uncertainty, which models the "unknown" in the plant in a specific manner. Typically encountered examples of structured uncertainty are gain and time constant or pole and zero uncertainty. If parametric uncertainty is used, a significant effort is required to produce the uncertain model. This is due to the requirement of an exact structure. Most analysis and design methods targeted for multivariable systems use state space models. For such models uncertainty is located at the level of some real parameters. In process control, these parameters are typically representing uncertainty in the model temperature, volume, flow, mass etc. It can be assumed that the model state space matrices depend linearly on these parameters. The $\mathcal{H}_\infty$ norm and the structured singular value (μ) are the main tools used for quantifying uncertainty in the frequency domain.

For multivariable (MIMO) systems, the concept of directions is prevalent. This is because, in MIMO systems, directions can lead to much higher sensitivity to uncertainty. At the same time for MIMO systems, deriving detailed uncertainty descriptions can lead to a significant effort. The curse of complexity extends over the non-parametric uncertainty representations for MIMO systems mainly because they give rise to full complex uncertainty transfer matrices which denote nonphysical couplings at the input or output of the plants. To solve this problem one can consider structured uncertainty in individual input channels (actuators) or output channels (sensors). This description maps into a diagonal structure for which the robustness analysis can be less conservative.

As a result, a general MIMO control configuration with uncertainty involves a block diagonal uncertainty matrix where each block represents either unstructured uncertainty (complex uncertainty) or structured uncertainty (captured by real deviation from a mean parameter value). By using in robust analysis a structured uncertainty transfer matrix not all uncertainty matrices are included, hence the level of conservativeness in the analysis is minimized.

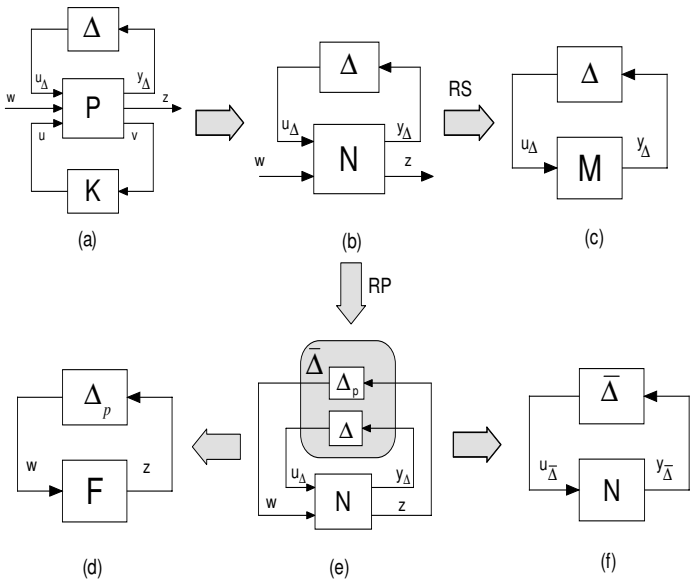

Fig. 2. Setting for robust stability (RS) and robust performance (RP), similar as in [8]

B. μ-analysis for robust stability

The concepts of robust stability and robust performance are illustrated in Figure 2 using the notation borrowed from [8]. The nominal plant P is described by

$$\begin{bmatrix} \begin{bmatrix} y_\Delta \\ z \end{bmatrix} \\ v \end{bmatrix} = \begin{bmatrix} P_{11} & P_{12} \\ P_{21} & P_{22} \end{bmatrix} \begin{bmatrix} \begin{bmatrix} u_\Delta \\ w \end{bmatrix} \\ u \end{bmatrix}.$$

The interconnection of P to a controller $u = Kv$ yields, as shown in Figure 2(b), the system $\begin{bmatrix} y_\Delta \\ z \end{bmatrix} = N \begin{bmatrix} u_\Delta \\ w \end{bmatrix}$, where N is defined by the lower Linear Fractional Transformation (LFT) of P and K:

$$N = F_l(P, K) = P_{11} + P_{12}K(I - P_{22}K)^{-1}P_{21}.$$

Also, observing Figure 2(d), $z = Fw$ and F is given by the upper LFT of N and Δ

$$F = F_u(N, \Delta) = N_{22} + N_{21}\Delta(I - N_{11}\Delta)^{-1}N_{12}.$$

Note that the nominal stability corresponds to the stability of N. For robust stability analysis, it is essential to check if the designed controller provides stability for all allowed plants. The plant in closed loop with Δ is $M = N_{11}$. Robust stability can be summarized as the stability of the $M\Delta$ interconnection in Figure 2(c) $\forall\Delta$ for which $\|\Delta\|_\infty \leq 1$. Equivalently, for robust stability, $F = F_u(N, \Delta)$ needs to be stable.

Robust stability for unstructured perturbations (*i.e.,* full block Δ) is equivalent to $\bar{\sigma}(M) < 1$, $\forall\omega$, which is equivalent to $||M||_\infty < 1$. For each perturbation block $\delta I = d_i\Delta_i d_i^{-1}$, which means $\Delta = D\Delta D^{-1}$, the robust stability condition boils down to $\bar{\sigma}(DMD^{-1}) < 1\ \forall\omega$. Since this applies to any $D = \mathrm{diag}(d_i)$ the updated robust stability condition is:

$$\min_{D(\omega)\in D} \bar{\sigma}(D(\omega)M(j\omega)D(\omega)^{-1}) < 1, \forall\omega$$

where D is the set of block diagonal matrices whose structure is compatible to that of Δ (i.e. $\Delta D = D\Delta$).

The structured singular value (SSV or μ) represents an essential tool used throughout both analysis and design. Let M be a complex matrix and let Δ_s be a set of complex matrices having the block diagonal structure $\mathrm{diag}(\Delta_i)$, specified by the sizes of Δ_i for $i = 1 \ldots k$. In this structure some of the blocks may be repeated and some may be restricted to be real. The structured singular value of M with respect to the structure Δ_s is defined by the real non-negative function

$$\mu_{\Delta_s}^{-1}(M) = \sup_{\Delta \in \Delta_s} \bar{\sigma}(\Delta) \text{ such that } det(I - M\Delta) \neq 0.$$

If no such Δ exists then $\mu_{\Delta_s}(M) = 0$. The subscript Δ_s may be dropped when the uncertainty structure is clear from the context. The above definition of μ extend to the case when the complex matrix M is frequency dependent, in which case, μ will also be frequency dependent.

Assume that the nominal system M and the perturbation Δ are stable, then the $M\Delta$ system is stable for all allowed perturbations with $\bar{\sigma}(\Delta) \leq 1$, $\forall\omega$ if and only if $\mu(M) < 1$, $\forall\omega$. Therefore the condition for robust stability for real or complex block diagonal perturbations may be rewritten as: Robust Stability $\Longleftrightarrow \mu(M(j\omega) < 1)$. These conditions may be interpreted also as the generalized small gain theorem that also takes into account the structure of Δ.

The structured singular value, a powerful tool for robust performance analysis, can also be employed for robust controller synthesis using the so-called DK-iteration procedure. The iterations are started with a stable $D(j\omega)$ with appropriate structure. The next step is to synthesize a controller for the scaled problem $\min_K(\min_{D\in\mathcal{D}} \|DN(K)D^{-1}\|_\infty)$. This step is followed by another find of an appropriate $D(j\omega)$ that minimizes at each frequency $\bar{\sigma}(DND^{-1})$ given a fixed N. Note that further a $D(j\omega)$ that is stable and minimum phase is propagated. Such iterations may continue until adequate performance is achieved. In this paper, we focus only on μ analysis and the aforementioned discussion on DK iteration was only offered for completeness.

C. μ-analysis for robust performance

For a control systems engineer ensuring robust stability of a designed loop is an essential step before attempting any practical implementation. The engineer efforts should never stop at this level since an equally important aspect of a successful control design is achieving closed loop performance. These notions have to be addressed simultaneously. Precisely, when performing control design nominal performance is important but, at the same time, accounting for plant uncertainty and providing expected performance across the whole operational envelope is mandatory. To observe if such goals were met the analysis of a closed loop involving a linear plant and controller can be pursued in the μ framework.

Robust performance of MIMO systems can also be addressed using the μ framework. Rearranging the system in the $N\Delta$ structure and assuming nominal stability (*i.e.,* N internally stable), the equivalent condition for robust performance (RP) is:

$$\begin{aligned} RP \quad &\Longleftrightarrow \quad \|F\|_\infty = \|F_u(N,\Delta)\|_\infty < 1, \forall \|\Delta\| \leq 1 \\ &\Longleftrightarrow \quad \mu_{\bar{\Delta}}(N(j\omega)) < 1, \forall\omega. \end{aligned}$$

The structured singular value is computed with respect to the structure $\bar{\Delta} = \begin{bmatrix} \Delta & 0 \\ 0 & \Delta_p \end{bmatrix}$ for which Δ_p is a full complex perturbation with the same dimensions as F (see Figure 2).

D. Worst-case uncertainty analysis using skewed μ

Insight into skewed μ can be gained by understanding the following example. Assuming that the peak μ value for a given closed loop design is 1.1. This means that the robust performance requirement will be satisfied exactly if we reduced both the performance requirement and the allowed uncertainty by 10 %. This shows that μ does not give the worst-case performance as one might have expected. To find the worst-case weighted performance for a given uncertainty one needs to keep the magnitude of the Δ perturbation fixed (i.e. $\bar{\sigma}(\Delta) \leq 1, \forall\omega$). In this case we need to compute the skewed μ of N defined as $\mu_S(N(j\omega)), \forall\omega = \max_{\bar{\sigma}(\Delta)\leq 1, \forall\omega} \|F_l(N,\Delta)(j\omega)\|_\infty$

III. μ Analysis Applied to Fuel Processor Control

We now describe the application of the theory in Section II to the CPO reactor temperature (T_{CPO}) control problem. The study is conducted using linear models derived from a high dimensional, nonlinear system level dynamic model [9]. The order of the linear model is reduced to a tractable size using the routines from the SLICOT library [10]. The μ computations are performed using the μ-Analysis and Synthesis Toolbox for MATLAB.

The control of T_{CPO} involves ensuring that the fuel and air flows are coordinated so that the oxygen-to-carbon (or equivalently, the air-to-fuel) ratio (O2C) is in an acceptable range. Excursions in O2C lead to high temperatures that damage the CPO catalyst. A second control objective that relates to fuel and air regulation is to meet the hydrogen demand from the fuel cell stack for producing the desired electrical power at prescribed hydrogen utilization. The overall control problem with both the objectives of H_2 utilization control and T_{CPO} control has been studied in [5], [6] where LQR and $\mathcal{H}_\infty$ techniques have been employed respectively. For simplicity, we restrict our attention in this paper to robustness analysis of the T_{CPO} loop only and ignore the hydrogen utilization part. This analysis can be easily extended to the case including the hydrogen utilization control.

The nominal closed loop system is shown in Figure 3. The power load is the external disturbance signal and the manipulated variables are the fuel valve open fraction and the air blower speed. We consider O2C as the performance variables since it captures both the temperature and the selectivity to H_2 in the CPO reactor. The measured variables used as feedback for the controller are the stack current, T_{CPO}, fuel flow and air flow.

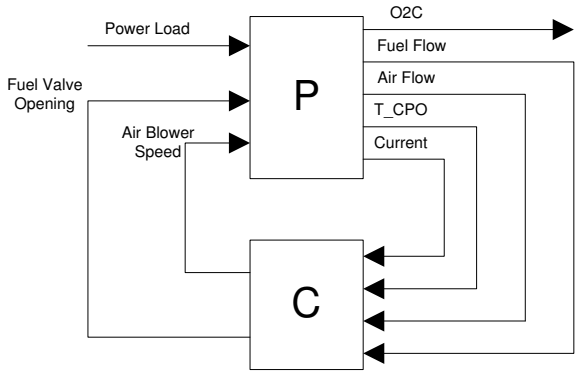

Fig. 3. Nominal closed loop system for the CPO reactor temperature control

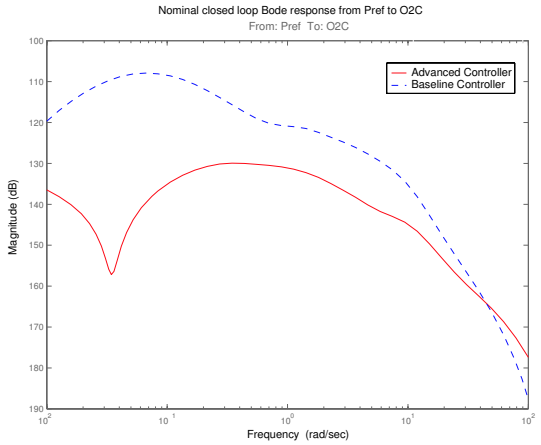

Fig. 4. Bode plot showing the nominal disturbance rejection performance of the baseline and the advanced controllers

We consider two controller architectures: the first one, a legacy controller, corresponds to the baseline case and has been designed using a decentralized approach. The second control architecture, which we refer to as the advanced controller, has been designed using multivariable design techniques described in [6]. A frequency domain comparison of the nominal disturbance rejection performance of the two controllers is shown in Figure 4 and it can be observed that the advanced controller gives better disturbance rejection as the gain for the advanced controller is well below that of the baseline controller.

A. Robust stability test

We now study the robust stability of the two controllers under structured, non-parametric uncertainty at the plant output. The disturbance signal (Power Load) and the performance output (O2C) are not relevant for the robust stability study. Multiplicative uncertainty in each of the three channels, namely, fuel flow, air flow and T_{CPO} is assumed.

The uncertainty weights for fuel and air flows are chosen as

$$W_1(s) = W_2(s) = 0.05\frac{2s+1}{s+1}$$

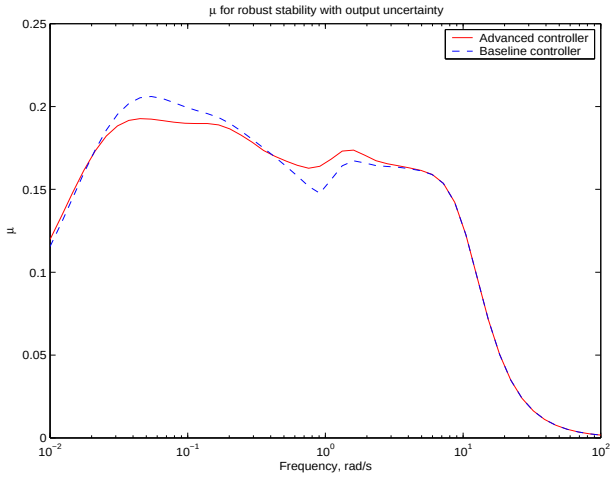

Fig. 5. Robust stability test: μ for the baseline (dashed line) and the advanced (solid line) controllers

which correspond to 5% uncertainty at steady state and 10% at high frequencies. The uncertainty weight for T_{CPO} is chosen as

$$W_3(s) = 0.05\frac{200s+1}{50s+1}$$

which corresponds to 5% at steady state and 20% at high frequencies. The block diagram of the system for the robust stability test is given by the upper LFT of N and Δ as in Figure 2 where N represents the nominal closed loop plant with the uncertainty weight $W = \mathrm{diag}(W_1, W_2, W_3)$ absorbed in and Δ is the structured uncertainty consisting of scalar uncertainty blocks $\Delta = \mathrm{diag}(\delta_1, \delta_2, \delta_3)$.

Robust stability of the system is guaranteed if the μ for the $N\Delta$ system is below unity for all frequencies. Moreover, the smaller the peak value of μ, the higher the robustness margin of the system. The μ computed for both the baseline controller and the advanced controller is shown in Figure 5. It can be seen that both controllers have robust stability to the prescribed level of uncertainty. The advanced controller has slightly smaller peak value of μ indicating better robust stability. In fact, if the uncertainty in T_{CPO} is higher or is at lower frequencies, the superiority of the advanced controller becomes prominent.

B. Robust performance test

In order to compare the robust performance of the baseline and the advanced controllers, we consider a slightly different setup. We introduce non-parametric multiplicative uncertainty in the fuel flow and air flow outputs with the weights given by

$$W_1(s) = W_2(s) = 0.05\frac{2s+1}{s+1}.$$

These weights correspond to 5% error at steady state and 10% error at high frequencies as in the robust stability test. The performance metric is the gain from the disturbance, Power Level, to the output, O2C. The weight for the performance

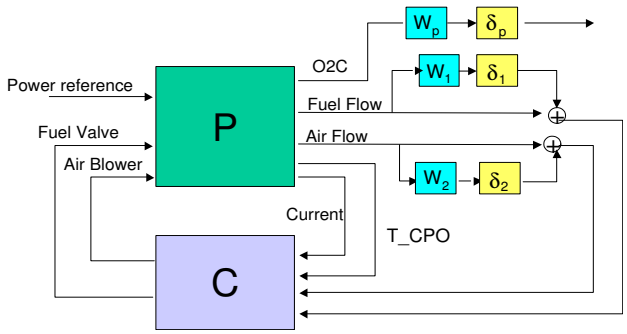

Fig. 6. Setting for robust performance study of the fuel processor controller

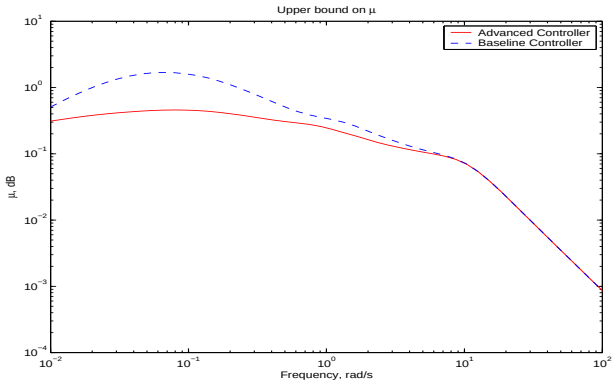

Fig. 7. Robust performance test: μ for the baseline (dashed line) and the advanced (solid line) controllers

variable is taken as

$$W_p = \frac{0.1}{\alpha}\frac{0.1s+1}{s+1}$$

where α is a scale factor that represents the desired steady state gain from the Power Level to O2C. Thus we, provide an allowance 10 times higher than the steady state allowance for O2C excursions during transients.

The block diagram of the system for the robust performance test is given by the interconnection of N and $\bar{\Delta}$ as in Figure 6 where N represents the nominal closed loop plant with the uncertainty weight $W = \mathrm{diag}(W_1, W_2, W_p)$ absorbed in and $\bar{\Delta}$ is the structured uncertainty consisting of scalar uncertainty blocks $\bar{\Delta} = \mathrm{diag}(\delta_1, \delta_2, \delta_p)$.

Robust performance of the system is guaranteed if the μ for the $N\bar{\Delta}$ system is below unity for all frequencies. Moreover, the smaller the peak value of μ, the higher the robustness performance margin of the system. That is, the system can tolerate higher level of model uncertainty without degradation in the disturbance rejection performance. The μ computed for both the baseline controller and the advanced controller is shown in Figure 7. It can be seen that the advanced controller has a peak μ less than unity and meets the robust performance requirement whereas the baseline controller has $\mu > 1$ and its robust performance is not guaranteed.

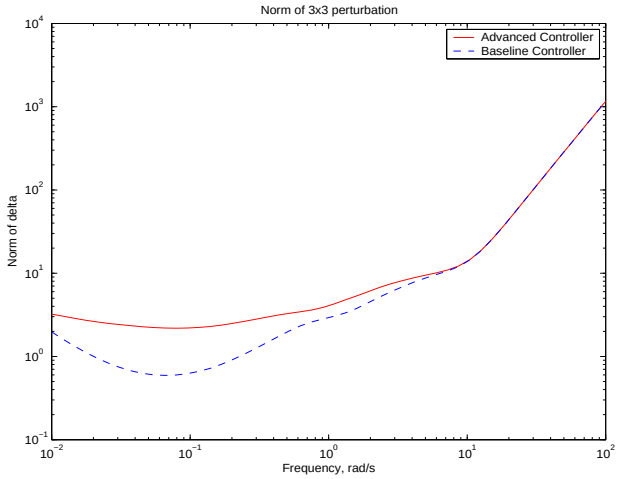

Fig. 8. Robust performance test: Norm of the destabilizing perturbation for the baseline (dashed line) and the advanced (solid line) controllers

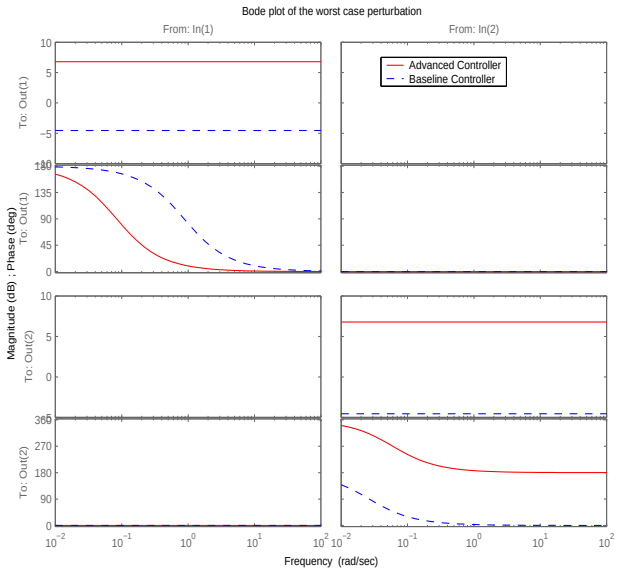

Fig. 9. Robust performance test: Bode plot of the worst case model uncertainty (2×2 Δ closed

The norm of the 3×3 perturbation (Δ) that makes the loop unstable is shown in Figure 8. The advanced controller can tolerate a larger Δ than the baseline controller.

The worst case Δ (2×2 model uncertainty) for the two controllers is shown in Figure 9. The advanced controller can tolerate larger uncertainty than the baseline controller.

The disturbance rejection performance (*i.e.*, the gain from power reference to O2C) with the 2×2 model uncertainty loop closed is shown in Figure 10. Again, it is evident that robustness of disturbance rejection is improved by the advanced controller.

C. Worst-case uncertainty test

As described in Section II-D, the skewed μ represents the true worst-case performance of an uncertain system. For the

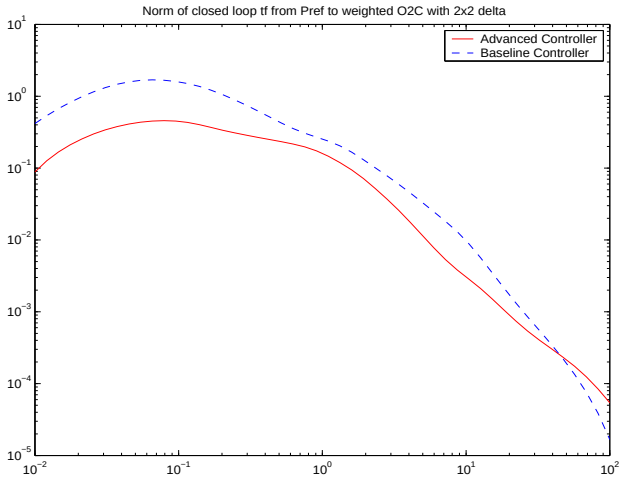

Fig. 10. Robust performance test: Disturbance gain (from power reference to O2C) with Δ (2×2 model uncertainty) loop closed

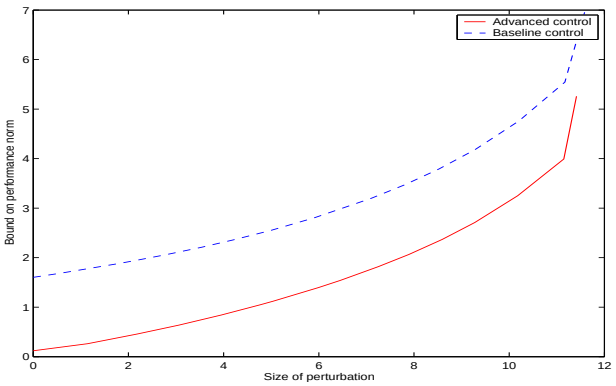

Fig. 11. Worst-case performance as a function of model uncertainty using skewed μ

system in Figure 6, we compute the worst-case disturbance rejection performance as a function of the size of model uncertainty in the flow measurements. Figure 11 shows the tradeoff between the size of the uncertainty (*i.e.*, the norm of the 2×2 Δ perturbation) and the worst-case performance for the baseline and the advanced controllers. It can be observed that the worst-case performance of the advanced controller is better than the baseline controller. It should also be noted that the nominal design of the advanced controller itself gives it an advantage in terms of superior disturbance rejection (see Figure 4).

IV. Conclusion

The CPO reactor temperature control problem in a fuel cell power plant was considered and the robust stability and robust performance of two different controllers under model uncertainty was evaluated using the μ-analysis framework. Linearized models derived from nonlinear system level dynamic models were employed for control analysis. The first controller (baseline) was a legacy controller designed using a decentralized approach. The second controller was designed using multivariable control design techniques. The robust stability of the closed loop system under the two controllers was compared when subjected to diagonal, structured, non-parametric uncertainty in the air flow, fuel flow and the temperature measurements. Robust performance of the two controllers was compared when subjected to structured, non-parametric uncertainty in the fuel and air flow measurements. Skewed-μ analysis was employed to evaluate the performance degradation as a function of model uncertainty for both the controllers. The analysis revealed that the advanced controller has better robustness properties than the baseline controller.

References

[1] J. Larminie and A. Dicks, *Fuel Cell Systems Explained*, 2nd ed. John Wiley & Sons, 2003.

[2] L. Carrette, K. A. Friedrich, and U. Stimming, "Fuel cells– fundamentals and applications," *Fuel Cells*, vol. 1, no. 1, pp. 5–39, 2001.

[3] A. K. Avci, D. L. Trimm, and Z. I. Onsan, "Quantitative investigation of catalytic natural gas conversion for hydrogen fuel cell applications," *Chemical Engineering Journal*, vol. 90, pp. 77–87, 2002.

[4] J. M. Zalc and D. G. Loffler, "Fuel processing for PEM fuel cells: transport and kinetic issues of system design," *Journal of Power Sources*, vol. 111, pp. 58–64, 2002.

[5] J. T. Pukrushpan, A. Stefanopoulou, H. Peng, S. Varigonda, L. M. Pedersen, and S. Ghosh, "Control of natural gas catalytic partial oxidation for hydrogen generation in fuel cell applications," *IEEE Trans. Contr. Syst. Tech*, (to appear).

[6] S. Varigonda, M. Kamat, and S. A. Bortoff, "H_∞ control design for a stationary fuel cell powerplant," in *Proc. of the IEEE CDC*, Bahamas, 2004, (submitted).

[7] K. Zhou, J. C. Doyle, and K. Glover, *Robust and Optimal Control*. Prentice Hall, 1996, chapter 13, Algebraic Riccati Equations.

[8] S. Skogestad and I. Postlethwaite, *Multivariable Feedback Control*. Wiley, 1996.

[9] J. Eborn, L. Pedersen, C. Haugstetter, and S. Ghosh, "System level dynamic modeling of fuel cell power plants," *Proceedings of the 2003 American Control Conference*, pp. 2024–2029, 2003.

[10] P. Benner, V. Mehrmann, V. Sima, S. Van Huffel, and A. Varga, *SLICOT– A Subroutine Library in Systems and Control Theory*. Birkauser, 1999, vol. 1, ch. 10, pp. 499–539. [Online]. Available: http://www.win.tue.nl/niconet/NIC2/slicot.html